Journal of Engineering Physics and Thermophysics, Vol. 81, No. 5, 2008

THEORETICAL AND EXPERIMENTAL INVESTIGATION OF THE CHARACTERISTICS OF A ROTARY-PULSATORY APPARATUS

V. M. Fomin,[a] **A. V. Fedorov,**[a]
T. A. Khmel',[a] **M. S. Vasilishin,**[b]
A. G. Karpov,[b] **and A. A. Kukhlenko**[b]

UDC 532.695

Experimental-theoretical investigation of the characteristics of a rotary-pulsatory apparatus with an impeller and controlled flow rate, which is intended to intensify the processes of extraction of substances from a vegetable raw material in the pharmaceutical industry, has been carried out. A semiempirical physicomathematical hydrodynamic model has been proposed; expressions for the characteristics of the averaged flow have been determined. Agreement between the calculated and experimental data on the head and the power consumption as functions of the flow-rate of the medium and the rotational velocity of the motor has been obtained.

Introduction. Improvement of the methods of intensification of mass-exchange processes in chemical and biochemical reactors on the basis of new physical principles is a topical scientific and technological problem. An important part of many chemical technologies is extraction. Extraction combined with simultaneous grinding of the raw material in rotary devices can turn out to be one efficient and widely used technique for extracting the desired product from substrates of different origin [1]. The use of rotary-pulsatory apparatuses (RPAs) for these purposes ensures high qualitative and quantitative indices of the process due to the specific hydrodynamic conditions created in RPAs: pressure pulsations, cavitation, vortex mixing, flow turbulization, and others.

Rotary-pulsatory apparatuses are developed and widely used for the production of finely dispersed emulsions and suspensions. Experimental and theoretical investigations of the characteristics of RPAs and the hydrodynamics of flows in the devices have been the focus of [2–8], including monographs [2, 3]. However, up to now, there have been no consistent ideas of the overall pattern of combined nonstationary three-dimensional flow of a liquid within the channels and radial clearances of RPAs. Consequently, all computational-theoretical models in designing such devices are based on empirical data. The dependences between the flow rate, the head, the rotational velocity of the rotor, and the power consumed by the device are important characteristics of an RPA.

The present work seeks to experimentally and theoretically analyze the operation of an apparatus of the rotary-pulsatory type which is fitted with an impeller and a flow governer and is developed for intensification of the process of extraction of substances from a vegetable raw material in the pharmaceutical industry.

Description of the Setup. The exterior view of a two-stage RPA is shown in Fig. 1. The working substance — a mixture of a ground vegetable raw material and an extragent — enters the device via the inlet central pipe, spins up to high revolutions using impeller vanes, then traverses the stator and rotor channels, and is removed via the outlet pipe. The stator and the rotor represent coaxial hollow cylinders on whose lateral surfaces there are channels for traversal of the substrate. The impeller has an inside diameter of 50 mm and contains 6 vanes of length 29 mm and height 17 mm at the periphery. The diameters of the inlet (suction) and outlet pipes are 32 and 27 mm, respectively.

[a]S. A. Khristianovich Institute of Theoretical and Applied Mechanics, Siberian Branch of the Russian Academy of Sciences, 4/1 Institutskaya Str., Novosibirsk, 630090, Russia; email: fedorov@itam.nsc.ru and khmel@itam.nsc.ru; [b]Institute of Problems of Chemical-Power Technologies, Siberian Branch of the Russian Academy of Sciences, Biisk, Russia. Translated from Inzhenerno-Fizicheskii Zhurnal, Vol. 81, No. 5, pp. 817–825, September–October, 2008. Original article submitted October 17, 2007.

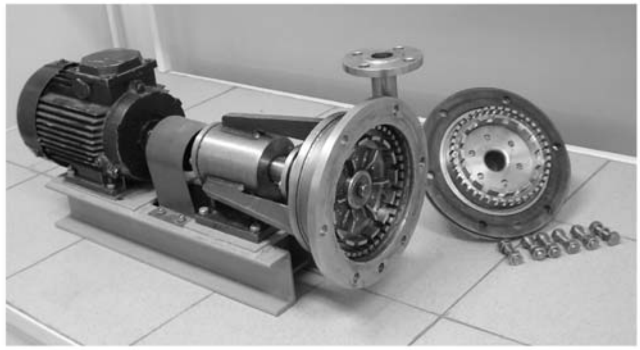

Fig. 1. Exterior view of the device.

TABLE 1. Parameters of the Stator–Rotor System in a Two-Stage RPA

Part of the device	Inside diameter, mm	Outside diameter, mm	Number of channels	Channel width, mm	Channel length, mm
Stator	114	124	15	10	15
internal external	142	152	40	5	16
Rotor	128	138	15	10	16
internal external	156	166	40	5	15

The characteristics of the stator and the rotor are given in Table 1. The channel length is the dimension in the axial direction, whereas the width is the dimension in the azimuthal direction.

The relative position of the stator and rotor channels changes in the operation of the apparatus; accordingly, the flow section for the substrate changes, too. Thus, flow in the apparatus is discontinuous and is characterized by high-frequency velocity and pressure pulsations. We note that in view of the limitations on transportation velocity, when readily inflammable liquids are used, the apparatus is directly connected to the governer limiting the flow rate. Such a device type differs from those considered in [6, 7] where the flow-rate characteristics were determined only by the rotational velocity of rotors and the rheological properties of the working substance.

Investigation of flows on an apparatus (Fig. 1) of the rotary-pulsatory type is a complex problem of the mechanics of heterogeneous media. The mixture of the extragent and the substrate treated represents an inhomogeneous two-phase medium with variance of the dimensions of inclusions and variable parameters. The motion of the mixture in the device is three-dimensional nonstationary and, generally speaking, does not possess axial symmetry both by virtue of the arrangement of vanes and because of the presence of the outlet pipe on the lateral surface. The presence of the system of channels uniformly arranged on the stator and rotor lateral surfaces determines the pulsatory character of flow with a frequency equal to the rotor's rotational frequency multiplied by the number of holes. Furthermore, stochastic pulsations due to both the inhomogeneity of the ground suspension and flow turbulization are possible.

In the initial step of theoretical and experimental investigations, we consider an incompressible liquid without inclusions (water) as the carrier medium. Trials of the devices include measurements of the hydrodynamic head and the power consumption for different values of the rotational velocity of the rotor and with variation of the guaranteed flow rate. We have proposed a semiempirical physicomathematical model within whose framework we investigated the hydrodynamics of flow in the device for theoretical analysis of the heat-flow-rate and energy characteristics of the RPA. A comparison of the results of theoretical calculations and experimental data makes it possible to determine the involved constants and to evaluate the field of applicability of the model.

Hydrodynamics of Flow within the RPA. The liquid in the RPA moves via the channels of the stator and the revolving rotor and via the clearances between the stator and the rotor. Within the channels, complex three-dimensional periodic vortex structures whose characteristics are determined mainly by the change in the flow section are realized. The characteristic dependences of the change in the internal flow section over a period for the device with two

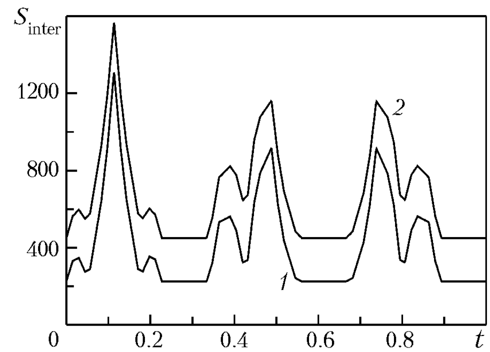

Fig. 2. Change in the area of the internal flow section of the device over a period. S_{inter}, mm^2.

stator–rotor stages are shown in Fig. 2. The maximum value of the flow section is attained when most of the rotor and stator channels are coincident; the minimum section is determined by the width of the radial clearances of the device.

Equations for the averaged velocity of traversal of the device by the liquid have been obtained in [3] by analysis of the tube of flow of an incompressible liquid and generalization of the Bernoulli equation to the case of nonstationary flow. The vortex character of flow within the stator and rotor channels has been suggested in [4]; however, the assumption of multiple rotation of the flow by an angle $\pi/2$ in traversal of the system of vortices has not been substantiated, we believe. The stability of flow in an analogous RPA has been investigated in [5]; Sorokina presented the flow pattern with a vortex system different from that in [4].

Without seeking to investigate flow within the RPA in detail, we attempt integral characteristics enabling us to evaluate the velocity of transportation of the liquid in the device. We consider the flow region including the volume of the stator and the rotor and the system of radial clearances between them. Equations describing three-dimensional nonstationary twisted flows of a viscous incompressible liquid have, in dimensionless variables, the following form:

$$\frac{\partial ur}{\partial r} + \frac{\partial vr}{\partial z} + \frac{1}{r}\frac{\partial wr}{\partial \theta} = 0 ,$$

$$\frac{\partial ur}{\partial t} + \frac{\partial u^2 r}{\partial r} + \frac{\partial uvr}{\partial z} + \frac{1}{r}\frac{\partial uwr}{\partial \theta} = - r\frac{\partial p}{\partial r} + w^2 + rf_r + \frac{1}{\text{Re}}\left[r\frac{\partial}{\partial r}\left(\frac{1}{r}\frac{\partial ru}{\partial r}\right) + \frac{\partial^2 ru}{\partial z^2} + \frac{1}{r^2}\frac{\partial^2 ru}{\partial \theta^2}\right],$$

$$\frac{\partial vr}{\partial t} + \frac{\partial uvr}{\partial r} + \frac{\partial v^2 r}{\partial z} + \frac{1}{r}\frac{\partial vwr}{\partial \theta} = - r\frac{\partial p}{\partial z} + rf_z + \frac{1}{\text{Re}}\left[r\frac{\partial}{\partial r}\left(\frac{1}{r}\frac{\partial rv}{\partial r}\right) + \frac{\partial^2 rv}{\partial z^2} + \frac{1}{r^2}\frac{\partial^2 rv}{\partial \theta^2}\right], \tag{1}$$

$$\frac{\partial wr}{\partial t} + \frac{\partial uwr}{\partial r} + \frac{\partial vwr}{\partial z} + \frac{1}{r}\frac{\partial w^2 r}{\partial \theta} = - uw - \frac{\partial p}{\partial \theta} + rf_\theta + \frac{1}{\text{Re}}\left[r\frac{\partial}{\partial r}\left(\frac{1}{r}\frac{\partial rw}{\partial r}\right) + \frac{\partial^2 rw}{\partial z^2} + \frac{1}{r^2}\frac{\partial^2 rw}{\partial \theta^2}\right]. \tag{2}$$

Here r, z, and θ are the radius, the axial (longitudinal) coordinate, and the angle. The liquid velocity in the volume filled with solid material is equal to zero. The influence of the walls (friction force and the force exerted by rotating surfaces) is modeled by introduction of a certain body force f.

For the device presented in Fig. 1, the recurrence period is 1/5 revolutions. The time of one cycle $T = 1/(5\Omega)$, where Ω is the rotational velocity of the rotor, is taken as the characteristics time of the pulsatory process in the apparatus. The circumferential rotational velocity of the rotor $W = 2\pi R\Omega$, where R is the mean radius of the stator–rotor combination, is taken as the velocity scale. Thus, the length scale is determined as $L = WT = 2\pi R/5$ and is equal to the distance between the coincident stator and rotor channels along the external-rotor circumstance. The Reynolds number of the system is $\text{Re} = 4\pi^2 R^2\Omega/5\nu$, where $\nu = \mu/\rho$.

An analysis of the parameters and the diagram of the device presented in Fig. 1 allows the assumption that the flows along the axis of rotation in the clearances and channels are weak. This property is determined by the location of the channels in the central part of the device and by their strictly radial arrangement in both the stator and the rotor. Therefore, in this step of investigation, we can also disregard motion in the z direction and the dependence of the parameters on z. Thus, the problem may be reduced to a two-dimensional one. We introduce the notation: D is the channel width in the azimuthal direction, H is the channel depth (total wall thickness of all the stator and rotor cylinders), and Z is the channel length (dimension along the axis of rotation). We take into account that the channel depth is much smaller than the stator and rotor radii, i.e., $H \ll R$. We introduce dimensionless quantities: $r_{\text{m}} = R/L$ is the mean radius of the stator–rotor system and $h = H/L$ is the relative depth of the channels in the device.

We determine the following integral characteristics:

$$\bar{u}(t) = \frac{1}{2\pi r_{\text{m}} h} \int_0^{2\pi} \int_{r_1}^{r_2} u(r, \theta, t)\, r dr d\theta, \qquad \frac{\overline{w^2}(t)}{r_{\text{m}}} = \frac{1}{2\pi r_{\text{m}} h} \int_0^{2\pi} \int_{r_1}^{r_2} \frac{w^2(r, \theta, t)}{r}\, r dr d\theta,$$

$$\bar{f}(t) = -\frac{1}{2\pi r_{\text{m}}} \int_0^{2\pi} \int_{r_1}^{r_2} f_r(r, \theta, t)\, r dr d\theta, \qquad \Delta p = \frac{1}{2\pi r_{\text{m}}} \int_0^{2\pi} \int_{r_1}^{r_2} \frac{r \partial p(r, \theta, t)}{\partial r}\, dr d\theta. \tag{3}$$

Here $\bar{u}(t)$ is the longitudinal velocity average over the internal volume of the stator and the rotor, $\overline{w^2}(t)$ is the mean value of the angular velocity squared ($\overline{w^2}(t) \neq [\overline{w}(t)]^2$, i.e., the twist squared is averaged); $\bar{f}(t)$ is the mean resistance force, and $r_1 = r_{\text{m}} - h/2$ and $r_2 = r_{\text{m}} + h/2$ are the internal and external radii of the stator–rotor system respectively. Integrating Eqs. (3) over the internal stator and rotor volume and disregarding the pulsatory component of the mean twist and the twist squared, we obtain, accurate to small values of the order of h, the following relation:

$$\frac{d\bar{u}(t)}{dt} - \frac{\overline{w}^2}{r_{\text{m}}} = -\frac{\Delta p}{h} - \frac{\bar{f}}{h}. \tag{4}$$

Thus, for the averaged flow (mean velocity of flow of the mixture in the device), the problem of determination of pulsatory motion in the apparatus is reduced to solution of an ordinary differential equation analogous to that obtained in [3]. We note that, unlike [3], in the present work, we give a successive derivation of the equation for the averaged flow in the RPA by averaging the complete equations describing nonstationary plane flow of the liquid.

To solve Eq. (1) we should redetermine the mean values of the circumferential velocity squared, the mean resistance force, and the mean applied pressure gradient.

Since the number and width of the stator and rotor channels are equal, we can assume that $\overline{w}^2 = 0.5$ for $H \ll R$. The resistance force is determined from the formula

$$\bar{f} = \frac{c_{\text{inter}} \bar{u}^2}{2} + \frac{\alpha \bar{u}^2}{2} + \beta \bar{u} h,$$

where c_{inter} is the pressure-loss factor in traversal of the system of convergent stator and rotor channels within the RPA by the liquid. For this factor, we take the formula [9, p. 408] of flow past grids with the contraction of the cross section:

$$c_{\text{inter}} = \frac{[0.707(1-\sigma)^{0.375} + 1 - \sigma]^2}{\sigma^2}, \quad \sigma = \frac{S_{\text{inter}}}{S^2}. \tag{5}$$

Here S_{inter} is the area of the internal flow section of the stator–rotor system and $S = 2\pi RZ$ is the mean area of the lateral surface of the stator–rotor system. The calculated dependences of the flow-section area on time are shown in Fig. 2. Curves 1 and 2 correspond to a clearance width of 1 mm (theoretical designed value) and 2 mm (maximum value with allowance for the error in treating the stator and rotor surfaces).

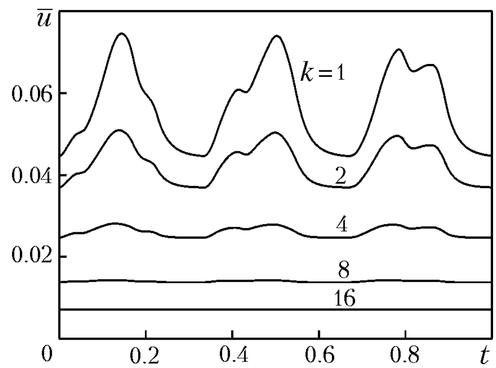

Fig. 3. Calculated profiles of the reduced transportation velocity for different degrees of limitation of the flow $h = 1/\sigma_v$.

The parameter α is determined from the formula of friction resistance in rough channels [9, p. 60] $\alpha = 0.5\lambda\sigma_{fr}$, where λ for the turbulent regime can roughly be taken to be 0.01 ([9], the plot on p. 62) and σ_{fr} is the ratio of the friction-surface area (product of the channel perimeter and length) to the flow section. As the evaluations show, we have $\alpha << \overline{c}_{inter}$ for the setup in question. The same is true of the filtration coefficient β expressing the linear friction loss. These quantities will be disregarded in what follows.

The applied pressure gradient for the device in question is

$$\Delta p = \Delta p_{imp} - \Delta p_{out} - \Delta p_v \, .$$

Here $\Delta p_{imp} = -\vartheta_{imp}(r^2_{imp,ext} - r^2_{imp,int})$ is ensured by the untwist of the flow by the impeller vanes ($r_{imp,ext}$, $r_{imp,int}$ are the dimensionless external and internal radii of the impeller) and ϑ_{imp} is the efficiency, which is determined empirically. The pressure loss on the outlet pipe of the device is $\Delta p_{out} = c_{out}\overline{u}^2/2$; the coefficient c_{out} is determined from the formula given in [9, p. 122–124]:

$$c_{out} = \frac{0.5\,(1 - \sigma_{out})}{\sigma^2_{out}}\,, \quad \sigma_{out} = \frac{S_{out}}{S}\,. \tag{6}$$

On the valve controlling the flow rate, we have $\Delta p_v = c_v\overline{u}^2/2$, where for the resistance coefficient, we take a formula analogous to formula (5) [9, p. 152]:

$$c_v = \frac{[0.707\,(1 - \sigma_v)^{0.375} + 1 - \sigma_v]^2}{(\sigma_{out}\sigma_v)^2}\,, \quad \sigma_v = \frac{S_v}{S_{out}}\,.$$

Figure 3 shows the calculated profiles of liquid-transportation velocity in the RPA for different degrees of valving off the section $k = 1/\sigma_v$. It is seen that not only does the mean value decrease with a considerable limitation in the flow rate but the pulsation amplitude decreases as well. Accordingly the transportation velocity becomes virtually time-independent (k = 8 and 16). We note that we are dealing only with the mean value of the radial velocity component; the azimuthal component is, as previously, characterized by intense pulsations in the process of traversal of the stator and rotor stages by the liquid in the devices.

Experimental Investigations of the RPA. A diagram of the test bench is shown in Fig. 4. The liquid-circulation loop is marked by a heavy line. A portion of the discharge line with heat exchanger 3 was not used in these experiments (it was cut off using the valve at the heat-exchanger inlet).

The flow rate was controlled by the valve just ahead of flow meter 4; the corresponding pressure in the discharge line was recorded by manometer 5. The pressure at the RPA inlet (suction line) was not specially measured with the manometer. According to evaluations, the static pressure component at the point of injection of the liquid into the RPA was in the interval 0.0079–0.0088 MPa for experimental conditions.

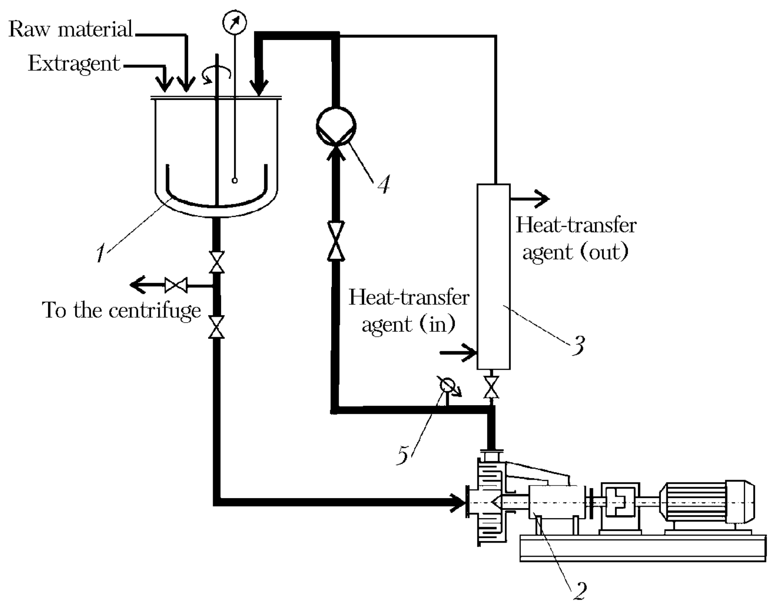

Fig. 4. Diagram of the test bench: 1) vessel with a mixing device; 2) RPA; 3) heat exchanger; 4) flow meter; 5) manometer.

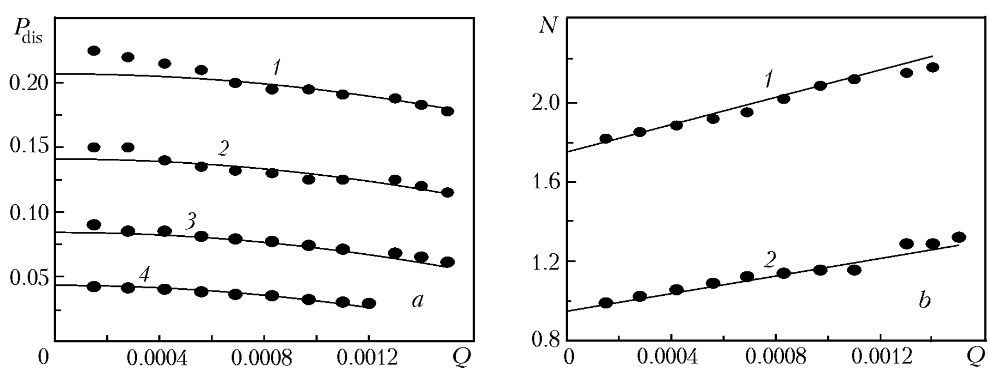

Fig. 5. Pressure in the discharge line (a) and power consumption (b) vs. flow rate: 1) Ω = 2885, 2) 2308, 3) 1731, and 4) 1124 rpm (points, experimental data, curves, calculation). P_{dis}, MPa; N, kW; Q, m^3/sec.

The results of measurements of the static pressure in the discharge line as a function of the flow rate for different values of the rotational frequency of the rotor are given in Fig. 5a. The power consumption of the motor was measured from the current strength. In view of the smallness of the latter, we did not reliably determine data on the motor power in the runs of tests at 1124 and 1731 rpm. Experimental values of the power consumption for rotational frequencies of the rotor of 2308 and 2885 rpm are marked in Fig. 5b.

Theoretical Analysis of Experimental Data. The maximum value of the flow rate under experimental conditions is restricted to a value of 0.0015 m^3/sec; therefore, the maximum mean transportation velocity is $U_{max} = Q_{max}/S = Q_{max}/(2\pi RZ) = 0.227$ m/sec, and the dimensionless value of $\overline{u}$ varies from 0.011 at 2800 rpm to 0.027 at 1154 rpm. According to the calculated results given in Fig. 3, the profiles are close to a constant function for these values of the mean velocity, which makes it possible to disregard transportation-velocity pulsations.

Next, for the sake of convenience, we will operate with capital-lettered dimensional quantities. It is noteworthy that the total pressure in the discharge line $P_{dis} + 0.5\rho U_{dis}^2$ is made up of the total inlet pressure $P_{in} + 0.5\rho U_{in}^2$ and the head ensured by the rotation of the impeller vanes P_{imp} and the rotation of the rotor P_{rot} minus the pressure loss by the internal resistance of the RPA ΔP_{inter} and the pressure loss on transition portions (ΔP_{in} in the inlet pipe and ΔP_{out} in the outlet pipe). Hence we have

$$P_{dis} = P_{in} + P_{imp} + P_{rot} - \Delta P_{inter} - \Delta P_{in} - \Delta P_{out} + 0.5\rho\,(U_{in}^2 - U_{dis}^2)\ . \quad (7)$$

Here each term is determined as follows. The inlet static pressure is P_{in} = 0.01 MPa under experimental conditions. The head produced by the centrifugal force of the liquid mass involved in rotation by the impeller vanes is $P_{imp} = \vartheta_{\text{ιμπ}}\rho(2\pi\Omega)^2/R^2_{imp,ext} - R^2_{imp,int})$. The pressure ensured by the rotation of the rotor stages is $P_{rot} = 0.4\rho(2\pi\Omega)^2 RH$ (for $H << R$). A coefficient of 0.4 expresses the ratio of the total area of the rotor channels to the area of the lateral rotor surface, since the centrifugal force is created only by the liquid mass in the channels of the device. The internal pressure loss is determined as $\Delta P_{inter} = \rho(2\pi R\Omega)^2\bar{c}_{inter}\bar{u}^2/2$, where $\bar{c}_{inter}$ is the time-average value of the internal resistance of the stator–rotor system. The liquid loss at entry into the outlet pipe due to the contraction of the flow section is equal to $\Delta P_{out} = 0.5(1 - S_{out}/S)\rho U_{out}^2/2$ [9, p. 151]. After substitution of the expressions for S and U_{out} with allowance for the relatively small diameter of the outlet pipe, we have

$$\Delta P_{out} \approx 0.5\rho\,(2\pi R\Omega)^2\left(\frac{2\pi RZ}{S_{out}}\right)^2\frac{\bar{u}^2}{2}\,.$$

Generally speaking, it is also necessary to take into account the pressure loss in passage of the liquid from the inlet pipe into the interior part of the device. The loss is difficult to determine, since direct use of the existing formulas for the pressure loss in tubes with expansion seems impossible, since the liquid is immediately involved in rotation and acquires centrifugal acceleration. We can only assume that the pressure loss at the device inlet is quadratically (with a certain coefficient) expressed by the mean transpormation velocity [9, pp. 146–147]:

$$\Delta P_{in} \approx \rho\vartheta_{in}U_{in}^2/2 = \rho\vartheta_{in}\,(2\pi R\Omega)^2\,(2\pi RZ/S_{in})^2\,\bar{u}^2/2\,,\quad \text{where}\ \vartheta_{in} < 1\,.$$

Primarily, we note that the limiting value of the pressure P_0 exists for low values of the flow rate (zero transportation velocity) (points in Fig. 6a). The curve in this figure is the dependence $P_0 = P_{in} + P_{imp0} + P_{rot} = P_{in} + A_0\Omega^2$ (the subscript 0 points to he value for the zero flow rate) obtained from formula (7). We take the coefficient A_0 = 93.6 Pa·sec^2 from the empirical data. From the formula $P_{imp0} + P_{rot} = \rho(2\pi\Omega)^2[\vartheta_{imp0}(R^2_{imp,ext} - R^2_{imp,int}) + 0.4RH]$, we determine the quantity ϑ_{imp0}. The maximum efficiency of the impeller is ϑ_{imp0} = 0.76 for this device. We note that the parabolic dependence of the head on the number of revolutions of the motor in the absence of continuous flow has also experimentally been obtained in [6].

For nonzero values of the flow rate, the discharge pressure is represented in the form

$$P_{dis} = P_{in} + P_{imp} + P_{rot} - 0.5\rho U^2\,(\bar{c}_{inter} + c_{out}) = P_{in} + P_{imp} + P_{rot} - A_P Q^2\ . \quad (8)$$

Here the constant $A_P = 0.5\rho(\bar{c}_{inter} + c_{out})/(2\pi RZ)^2$ is independent of the rotation of the rotor and the flow rate.

Figure 5a shows, by the lines, the calculated values determined from formula (8) for the impeller efficiency ϑ_{imp} = 0.68, where the resistance coefficients are determined from formulas (5) and (6) and the resistance on the inlet portion for the nonzero flow rate is disregarded. The best agreement between the experimental and calculated data has been obtained for the RPA internal resistance $\bar{c}_{inter}$ = 1100, whence σ = 0.04, which corresponds to a mean value of the RPA internal flow section of 280 mm^2 and is consistent with the dependence $S_{inter}(t)$ (curve 1) presented in Fig. 2. As is seen in Fig. 5a, the agreement between the calculated and experimental data for small revolutions (curves 3 and 4) is ensured virtually throughout the Q range. For Ω = 2308 rpm, change to the value ϑ_{imp} = 0.76 occurs for $Q < 0.0004$ m^3/sec (the points and curve 2 are compared), whereas for Ω = 2308 rpm the impeller efficiency smoothly decreases from a value of 0.76 when Q = 0 to 0.68 when $Q \approx 0.0006$ m^3/sec (the points and curve 1 are compared). We note that the same pair of values (ϑ_{imp} and σ) ensures good agreement with the entire set of experimental data for different values of the rotational velocity of the rotor.

The parabolic dependence of the head on the medium's flow rate in an RPA was obtained experimentally and was confirmed theoretically in [4], too. However, we note that the device considered in [4] was not fitted with an impeller and gave very low flow rates (to 0.0003 m^3/sec).

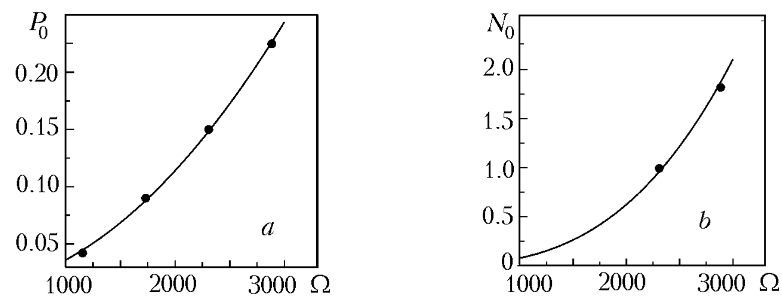

Fig. 6. Limiting values of pressure (a) and power (b) for disappearing flow rate vs. rotational velocity of the rotor. P_0, MPa; N_0, kW; Ω, rpm.

An important characteristic of the apparatuse is the power N consumed in operation of the RPA. It is made up of the power expended for the zero flow rate N_0 on accelerating the flowing liquid by vanes N_{imp} and in the rotor N_{rot} and on overcoming all resistance forces in transportation of the liquid N_{fr} (forces of internal resistance of the RPA, resistance in the inlet and outlet pipes, and resistance on the control valve):

$$N = N_0 + N_{\text{imp}} + N_{\text{rot}} + N_{\text{fr}} \,.$$

The quantity N_0 includes the no-load power of the motor and the power to overcome the moment of resistance in rotation of the impeller and the rotor. According to the existing representations for rotary devices (fans, etc.), the quantity N_0 is related to the angular rotational velocity by the dependence $N_0 = A_0\Omega^3$. The experimental limiting values (points in Fig. 6b) are in complete agreement with the above law (curve).

The power expended on untwisting the entering liquid by impeller vanes and in the rotor channels can be evaluated as

$$N_{\text{imp}} + N_{\text{rot}} = \eta_{\text{imp}}\rho\,(2\pi R_{\text{imp,ext}}\Omega)^2\,Q + 2\eta_{\text{rot}}\rho\,(2\pi R\Omega)^2\,Q \,, \tag{9}$$

where η_{imp} and η_{rot} are the coefficients reflecting the degree of involvement of the liquid flowing through the vanes and the rotor channels in rotation.

The power expended on overcoming all the resistance forces in transportation of the liquid is

$$N_{\text{fr}} = 0.5\rho U^2\,(c_{\text{inter}} + c_{\text{out}} + c_{\text{v}})\,Q \,. \tag{10}$$

Here the quantity to be determined is the valve resistance, since the flow section on the valve changes for each pair of values (rotational velocity–flow rate); however, this characteristic has not been measured. We assume that the valve resistance counterbalances the discharge pressure, i.e., we apply the Bernoulli theorem to the conditions at the device inlet and at the valve outlet. Then, with account for dependence (8) and disregarding the difference in velocity in the inlet and outlet pipes, we obtain $N_{\text{fr}} \approx (P_{\text{imp}} + P_{\text{rot}})Q$. Finally, the power consumption is represented by a polynomial of the form $N = N_0(\Omega) + A_N\Omega^2 Q$. The corresponding curves are shown in Fig. 5b. The constant A_N from empirical data is determined to be 0.15 kW·sec^3/m^3, which allows an estimate, within reasonable limits, of 0.3–0.4 for η_{rot}. As is seen in Fig. 5b, the behavior of the experimental points is in good agreement with theoretical representations.

Conclusions. In the work, we have experimentally and theoretically investigated the characteristics of an RPA with an impeller and controlled flow rate. We have established the experimental dependences of the head and the power consumption on the flow rate of the liquid for different rotational velocities of the rotor. We have proposed a semiempirical mathematical model making it possible to describe the averaged flow and to obtain expressions for the basic characteristics. We have determined the involved constants of the model, which ensure good agreement between the theoretical curves and the entire set of reliable experimental data. A certain deviation from the parabolic curves in the dependences of the head on the flow rate is related to the change in the impeller efficiency with appearance of continuous flow.

NOTATION

A, coefficient in the linear dependence; *c*, resistance coefficient; *D*, channel width, m; *f*, force; *h*, relative channel depth; *H*, channel depth, m; *k*, degree of valving-off; *L*, length scale, m; *N*, power, W; *P*, pressure, Pa; *p*, dimensionless pressure; *Q*, flow rate, m^3/sec; *R*, radius, m; *r*, dimensionless radius; *S*, free section, m^2; *T*, period, sec; *t*, time; *U*, transportation velocity, m/sec; *u*, *v*, and *w*, radial, axial, and azimuthal velocity components; *W*, circumferential velocity, m/sec; *Z*, channel length, m; *z*, θ, cylindrical coordinates; α, β, and λ, coefficients in the formulas for resistance; η, coefficient of involvement in rotation; ϑ, efficiency; μ, dynamic viscosity, kg/(m·sec); ν, kinematic viscosity, m^2/sec; ρ, density, kg/m^3; σ, coefficient of contraction of the flow section; Ω, rotational velocity of the rotor, 1/sec. Subscripts: 0, for the zero flow rate; 1 and 2, internal and external in the stator–rotor system; *r*, *z*, and θ, components in cylindrical coordinates; max, maximum; v, valve; int, internal for the impeller; inter, internal for the device; in, inlet pipe; out, outlet pipe; imp, impeller; ext, external for the impeller; dis, in the discharge line; rot, rotor; m, mean in the stator–rotor system; fr, friction.

REFERENCES

1. M. A. Promtov, *Machines and Apparatuses with Pulse Power Effects on Treated Substances* [in Russian], Mashinostroenie, Moscow (2004).
2. A. I. Zimin, *Applied Mechanics of Discontinuous Flows* [in Russian], Foliant, Moscow (1997).
3. A. M. Balabyshko, A. I. Zimin, and V. P. Ruzhitskii, *Hydromechanical Dispersion* [in Russian], Nauka, Moscow (1998).
4. A. I. Nakorchevskii, B. I. Basok, and T. S. Ryzhkova, Hydrodynamics of rotary-pulsatory apparatuses, *Inzh.-Fiz. Zh.*, **75**, No. 2, 58–68 (2002).
5. T. V. Sorokina, Hydrodynamic instability in rotary-pulsatory apparatuses, *Prom. Teplotekh.*, **26**, No. 6, 80–82 (2004).
6. I. A. Pirozhenko, Experimental investigations of the thermal and hydrodynamic characteristics of a liquid in a rotary-pulsatory apparatus, *Prom. Teplotekh.*, **26**, No. 6, 106–113 (2004).
7. Yu. S. Kravchenko, B. I. Basok, B. V. Davydenko, and I. A. Pirozhenko, Influence of the viscosity of a treated medium on the dynamic characteristics of a rotary-pulsatory apparatus, *Prom. Teplotekh.*, **26**, No. 1, 7–11 (2004).
8. Yu. A. Gostev, A. V. Fedorov, V. M. Fomin, T. A. Khmel', *On Two Problems of the Mechanics of Heterogeneous Media*, Preprint No. 3-2006 of the S. A. Khristianovich Institute of Theoretical and Applied Mechanics, Siberian Branch of the Russian Academy of Sciences, Novosibirsk (2006).
9. I. E. Idel'chik, *Handbook of Hydraulic Resistances* [in Russian], Mashinostroenie, Moscow (1992).